Supporting Information

for

Interplay between Ruthenium Sensitizer and Ruthenium Catalyst in Photoelectrochemical Cells with Different Water-Based Electrolytes

Iwona Grądzka-Kurzaj [a *], Mateusz Gierszewski [a],
Gotard Burdziński [a], Marcin Ziółek [a *]

[a] Faculty of Physics, Adam Mickiewicz University in Poznań,
Uniwersytetu Poznańskiego 2, 61-614 Poznań, Poland.

* corresponding authors: iwona.gradzka@amu.edu.pl (I. G.-K.), marziol@amu.edu.pl (M. Z.)

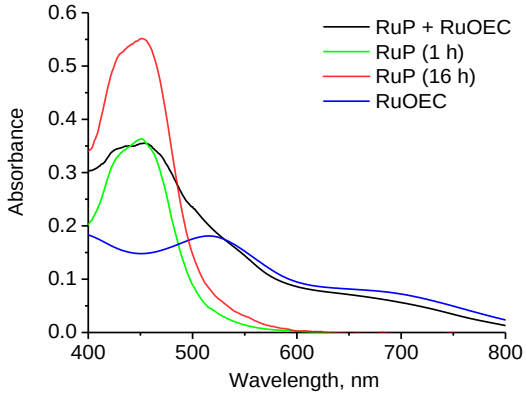

Figure S1. Absorption spectra of TiO_2-based photoanodes sensitized in RuP (for 1 h), RuP (for 16 h), RuOEC (for 16 h) and with both: RuP for (1 h) and then in RuOEC (16 h). TiO_2 contribution is subtracted.

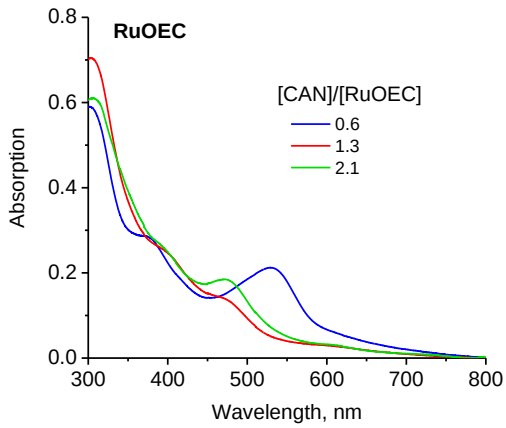

Figure S2. Spectrophotometric redox titration of RuOEC with ceric ammonium nitrate (CAN).

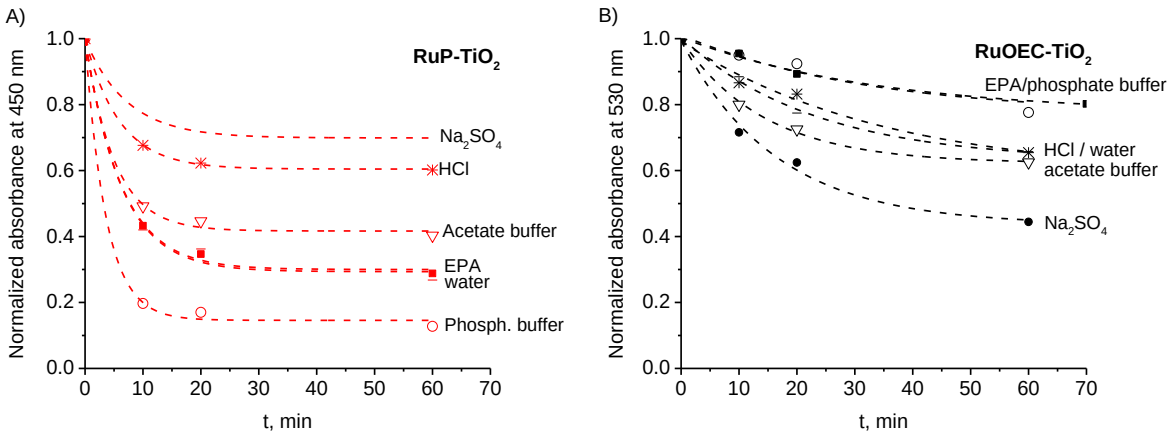

Figure S3. Changes in the absorption spectrum of RuP A) and RuOEC B) on TiO_2 in aqueous electrolyte.

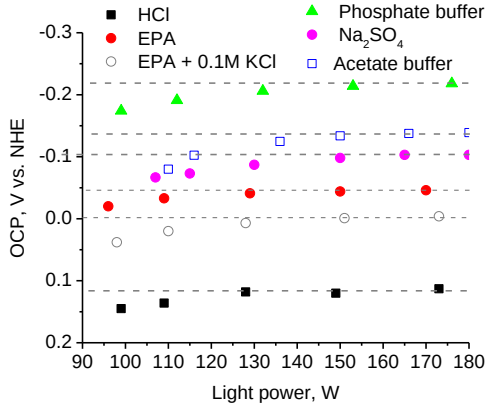

Figure S4. Open circuit potential of TiO_2 in different electrolytes plotted versus light supply power (proportional to the illumination intensity).

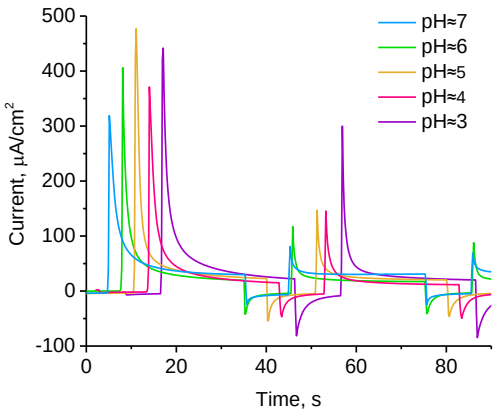

Figure S5. Photocurrent-time behaviour of RuP/RuOEC-TiO_2 in 0.7 M phosphate buffer in different pH (pH adjusted with EPA).

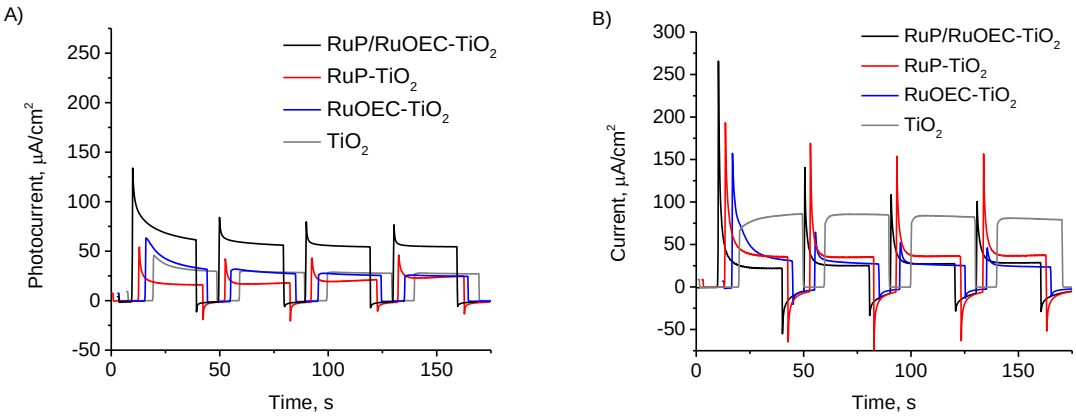

Figure S6. Photocurrent-time behaviour of TiO_2 sensitized with ruthenium compounds in A) phosphate buffer and B) in acetate buffer. The photoanodes were biased at 0.236 V vs. NHE.

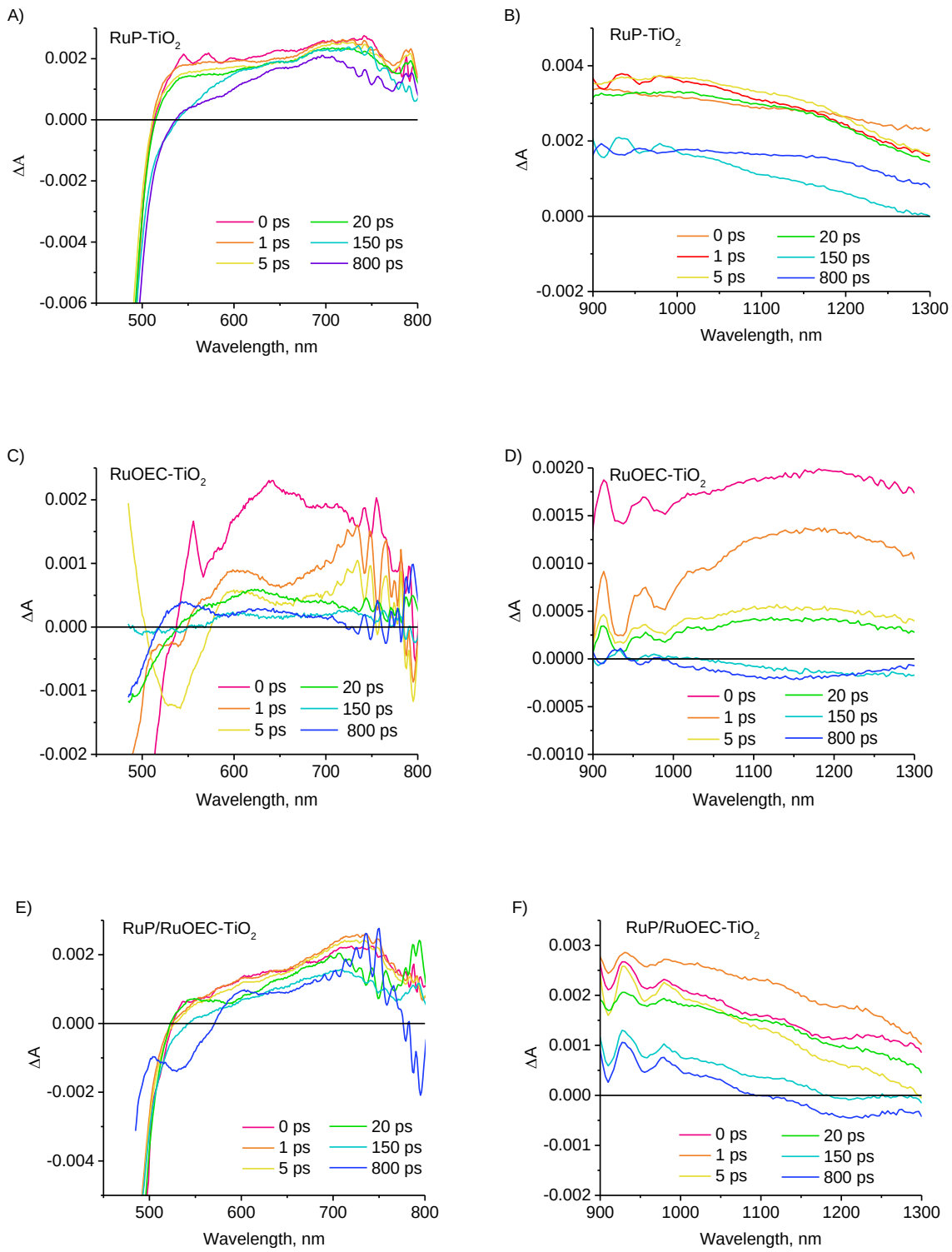

Figure S7. Transient absorption spectra of TiO_2 photoanodes sensitized with A), B) RuP, C), D) RuOEC and both E), F) RuP and RuOEC at different delay times. Conditions: two-electrode DSPEC filled with 0.1 M Na_2SO_4.

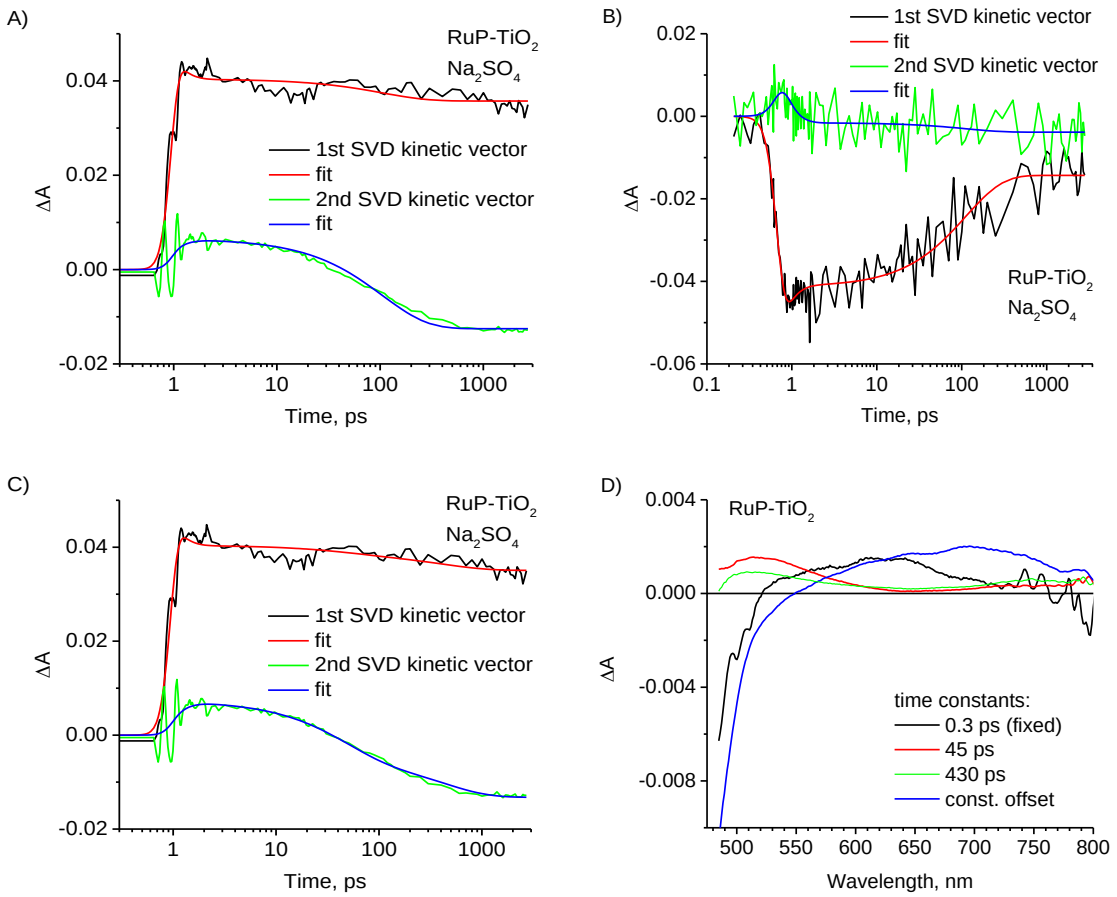

Figure S8. Examples of the global fits of a 2-exponential (fixed 0.3 ps + free component + constant offset) to the kinetic vectors obtained from singular value decomposition (SVD) of the transient absorption data recorded in A) VIS and B) NIR. C) Example of the global fits of a 3-exponential (fixed 0.3 ps + 2 free components + constant offset) to the same kinetic vectors VIS range. D) Wavelength dependent amplitudes corresponding to the global fit in C). The analysed spectrum was recorded for RuP-TiO_2 in Na_2SO_4 in all graphs.

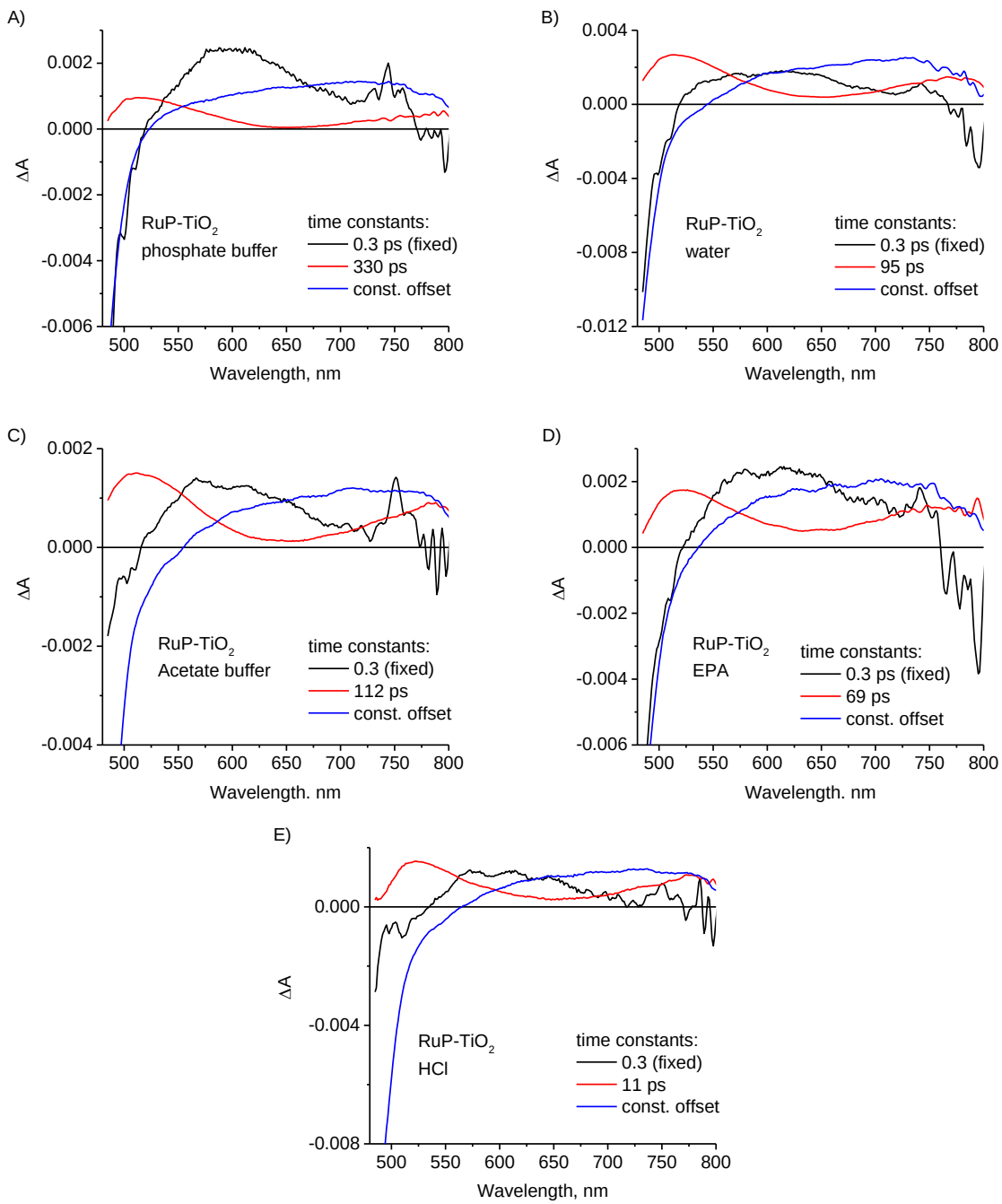

Figure S9. Wavelength-dependent amplitudes of the fitted time components for RuP-TiO_2 in A) water, B) phosphate buffer, C) acetate buffer, D) EPA, E) HCl.

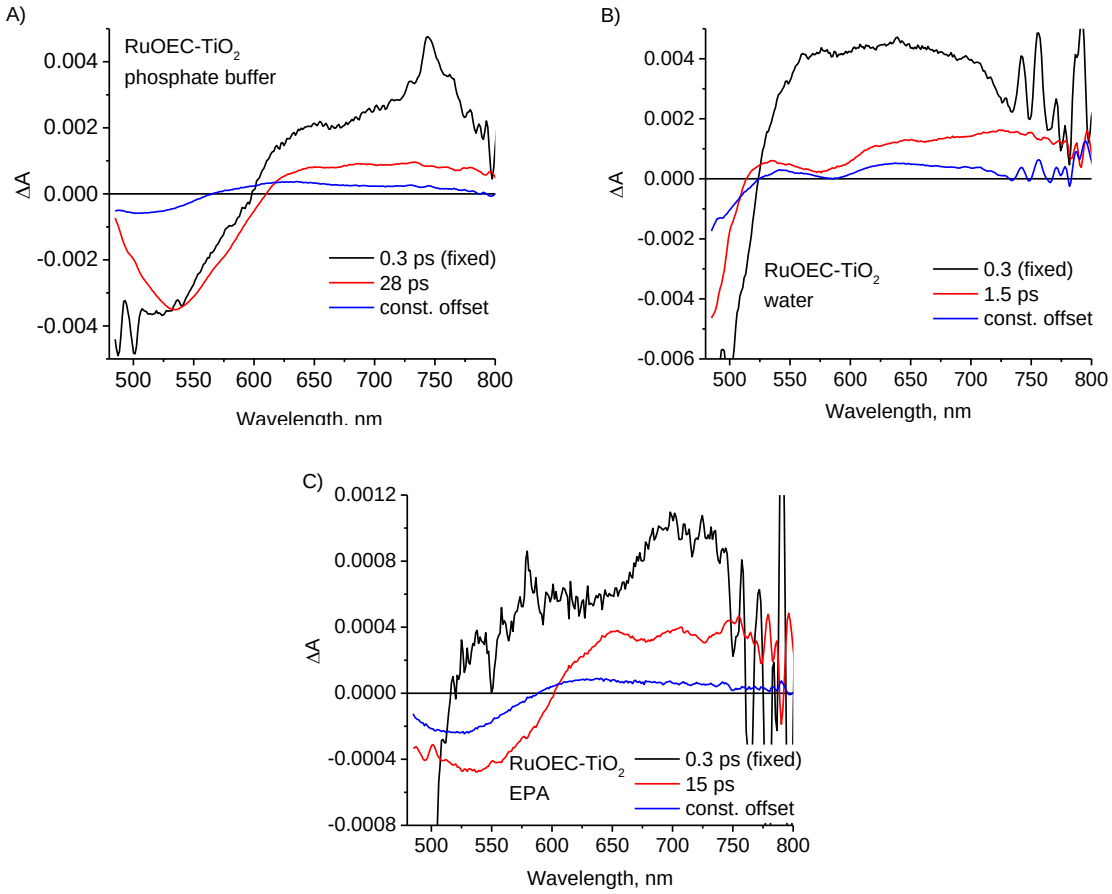

Figure S10. Wavelength-dependent amplitudes of the fitted time components for RuOEC-TiO_2 in A) phosphate buffer, B) water, C) EPA.

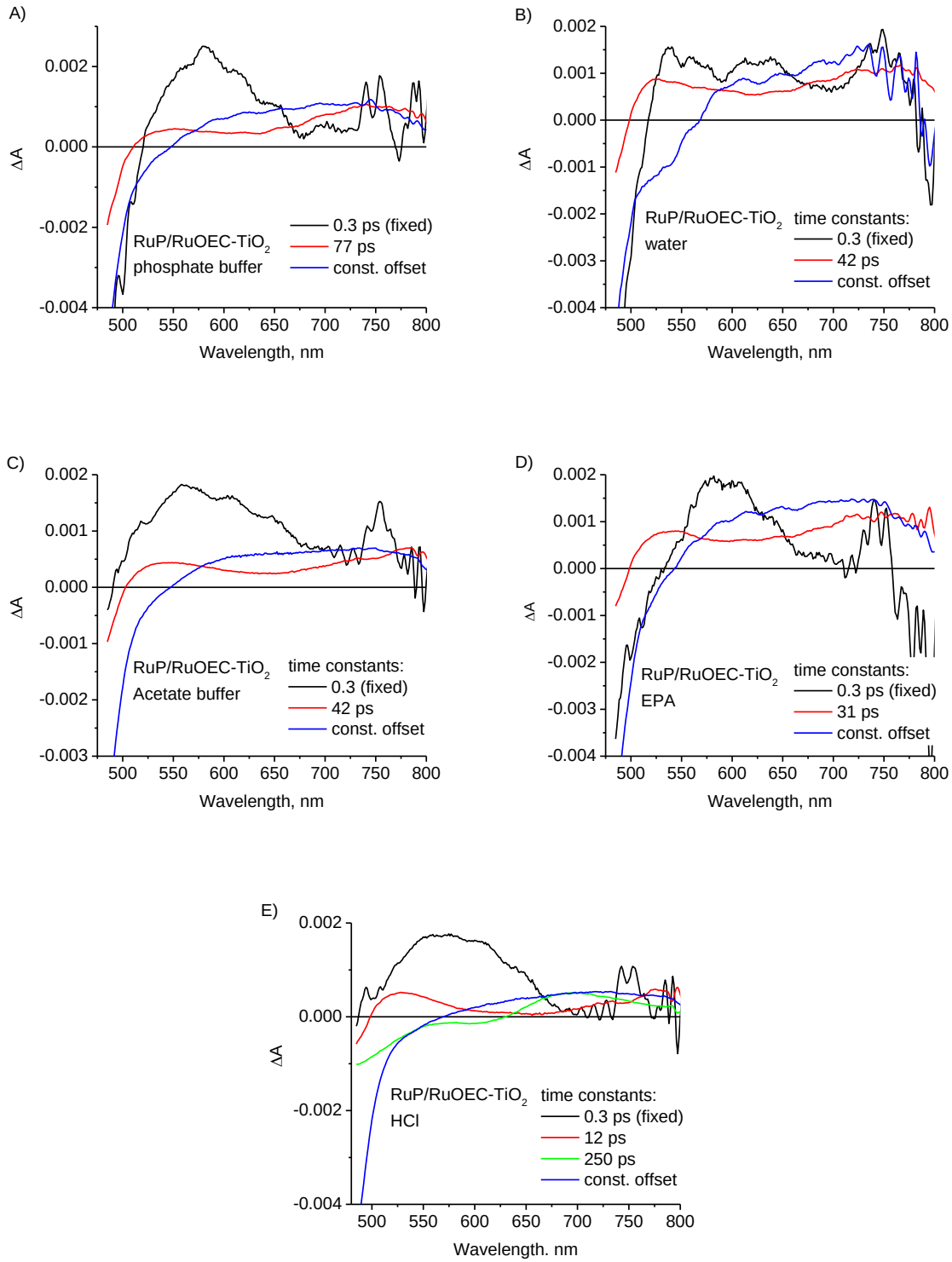

Figure S11. Wavelength-dependent amplitudes of the fitted time components for RuP/RuOEC-TiO_2 in A) phosphate buffer, B) water, C) acetate buffer, D) EPA, E) HCl.

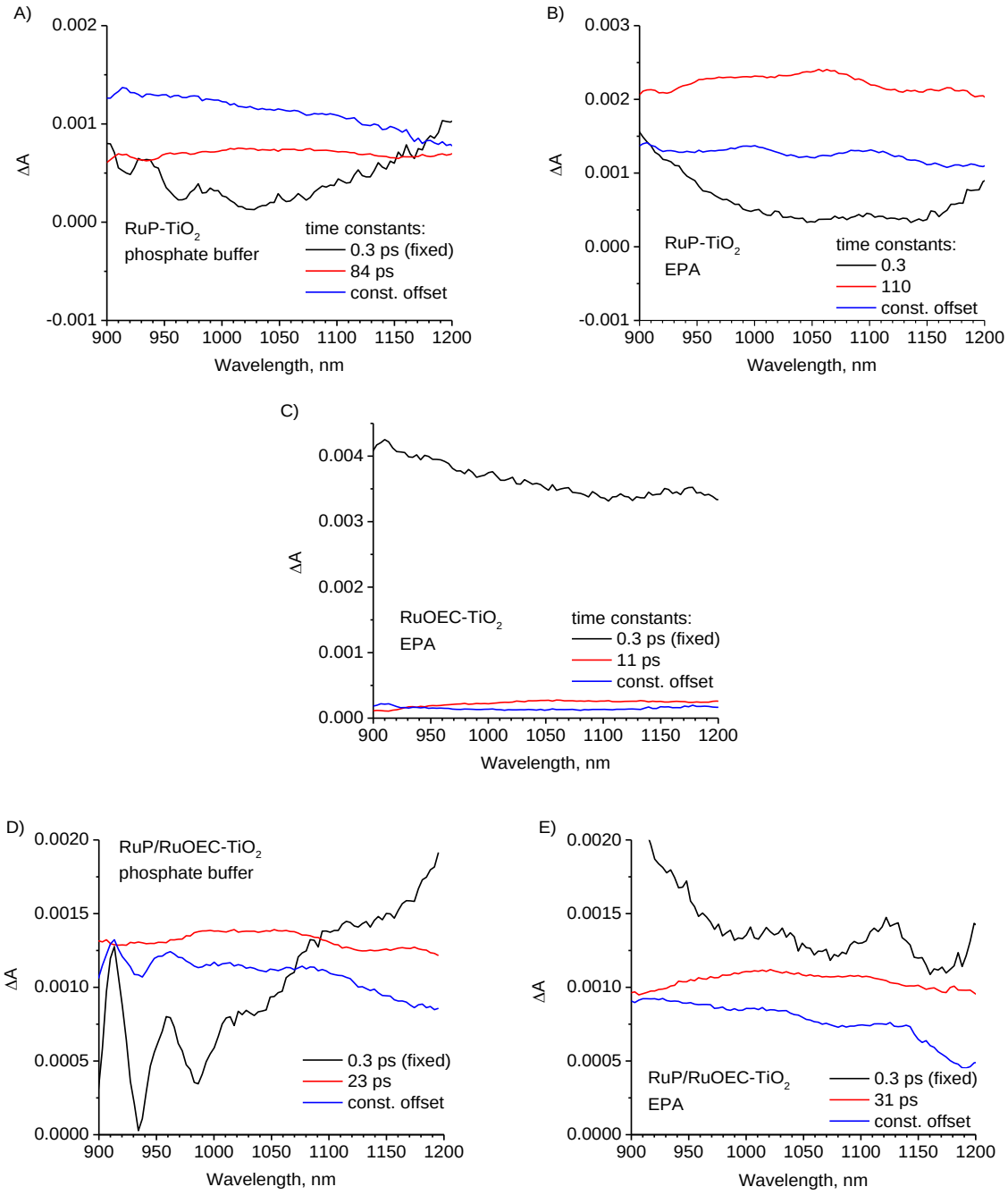

Figure S12. Wavelength-dependent amplitudes of the fitted time components obtained from global analysis of transient absorption spectra recorded in NIR range of RuP-TiO_2 in A) phosphate buffer, B) EPA, C) RuOEC-TiO_2 in EPA, and RuP/RuOEC-TiO_2 in D) phosphate buffer, E) EPA.

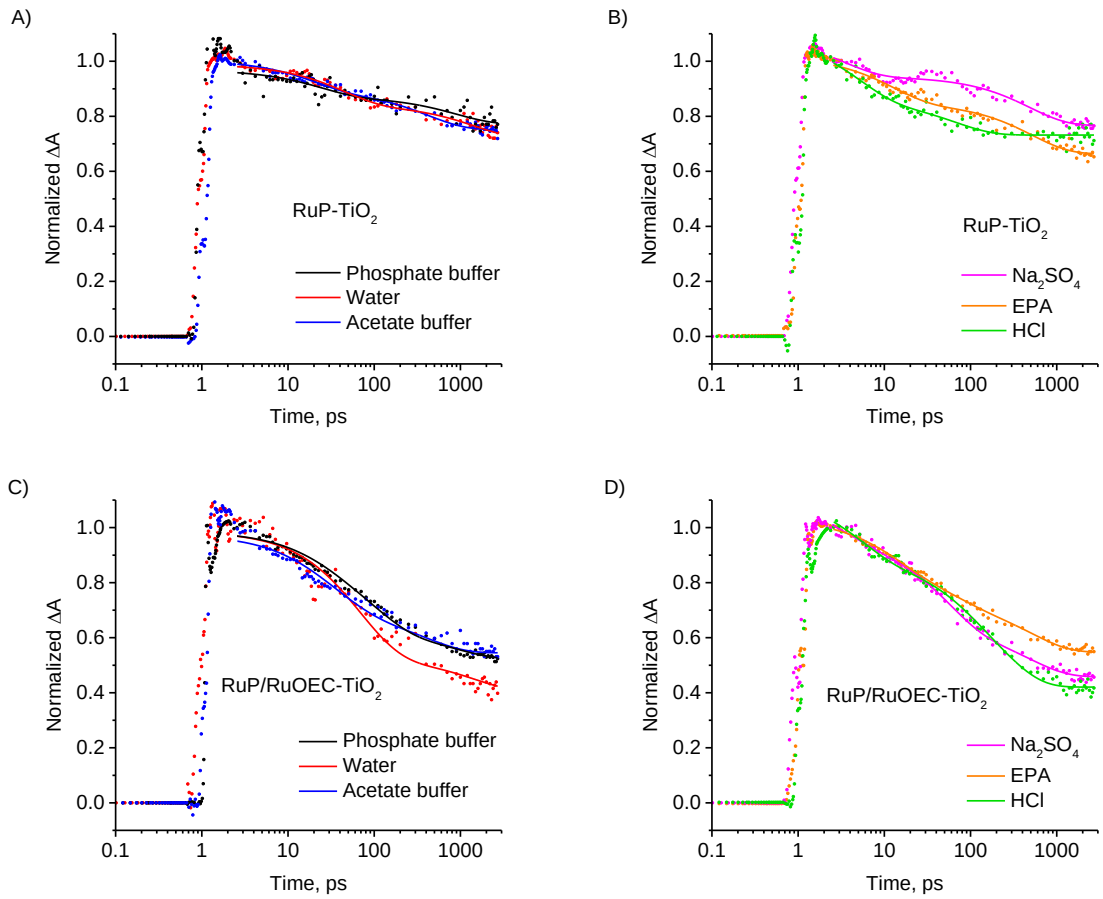

Figure S13. Transient absorption kinetics (dotted lines) at 700 nm for A) B) RuP-TiO_2 and C) D) RuP/RuOEC-TiO_2 with multiple exponential decay fits (solid lines), in different electrolytes. The kinetics are normalized to the signal recorded at 2.6 ps. Time zero was shifted to 1.5 ps to present the kinetics in the logarithmic scale.

Table S1. Parameters of multiexponential decay fitted to RuP-TiO_2 kinetic traces at 700 nm from femtosecond transient absorption.

RuP-TiO_2	Phosphate buffer	Water	Acetate buffer	Na_2SO_4	EPA	HCl
pH	pH ~7.1	pH ~6.5	pH ~4.5	pH ~6.5	pH ~3	pH ~3
x0, ps	2.6	2.6	2.6	2.6	2.6	2.6
y0	0.77	0.72	0.75	0.77	0.66	0.73
A1	0.09	0.14	0.10	0.07	0.14	0.14
t1, ps	24 ± 9	44 ± 7	20 ± 4	3 ± 1	12 ± 2	5 ± 1
A2	0.10	0.12	0.14	0.18	0.18	0.12
t2, ps	896 ± 212	1456 ± 177	422 ± 66	489 ± 61	518 ± 75	67 ± 16

Table S2. Parameters of multiexponential decay fitted to RuP/RuOEC-TiO_2 kinetic traces at 700 nm from femtosecond transient absorption.

RuP/RuOEC-TiO_2	Phosphate buffer	Water	Acetate buffer	Na_2SO_4	EPA	HCl
	pH ~7.1	pH ~6.5	pH ~4.5	pH ~6.5	pH ~3	pH ~3
x0, ps	2.6	2.6	2.6	2.6	2.6	2.6
y0	0.52	0.30	0.55	0.46	0.54	0.55
A1	0.09 (fixed)	0.14 (fixed)	0.10 (fixed)	0.07 (fixed)	0.14 (fixed)	0.14
t1, ps	24 (fixed)	44 (fixed)	20 (fixed)	3 (fixed)	12 (fixed)	5
A2	0.10 (fixed)	0.12 (fixed)	0.14 (fixed)	0.18 (fixed)	0.18 (fixed)	0.12
t2, ps	896 (fixed)	1456 (fixed)	422 (fixed)	489 (fixed)	518 (fixed)	67
A3	0.26	0.30	0.16	0.30	0.12	0.34
t3, ps	**104 ± 20**	**87 ± 12**	**50 ± 6**	**52 ± 3**	**58 ± 5**	**250 ± 13**

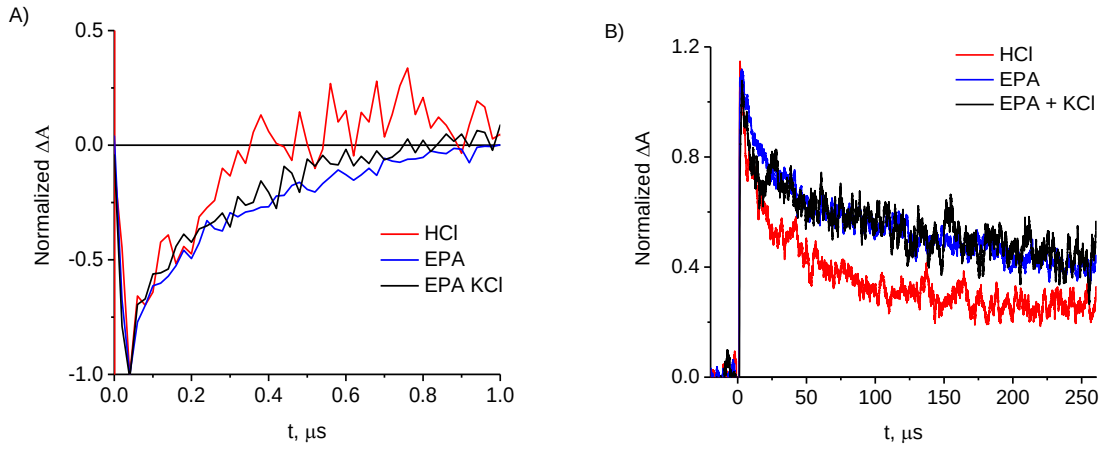

Figure S14. Kinetics at 700 nm (normalized at peaks) obtained in flash photolysis for the RuP-TiO_2 samples in EPA, HCl and EPA + 0.1 M KCl (all pH ~3) in A) negative signal and B) positive signal time region.

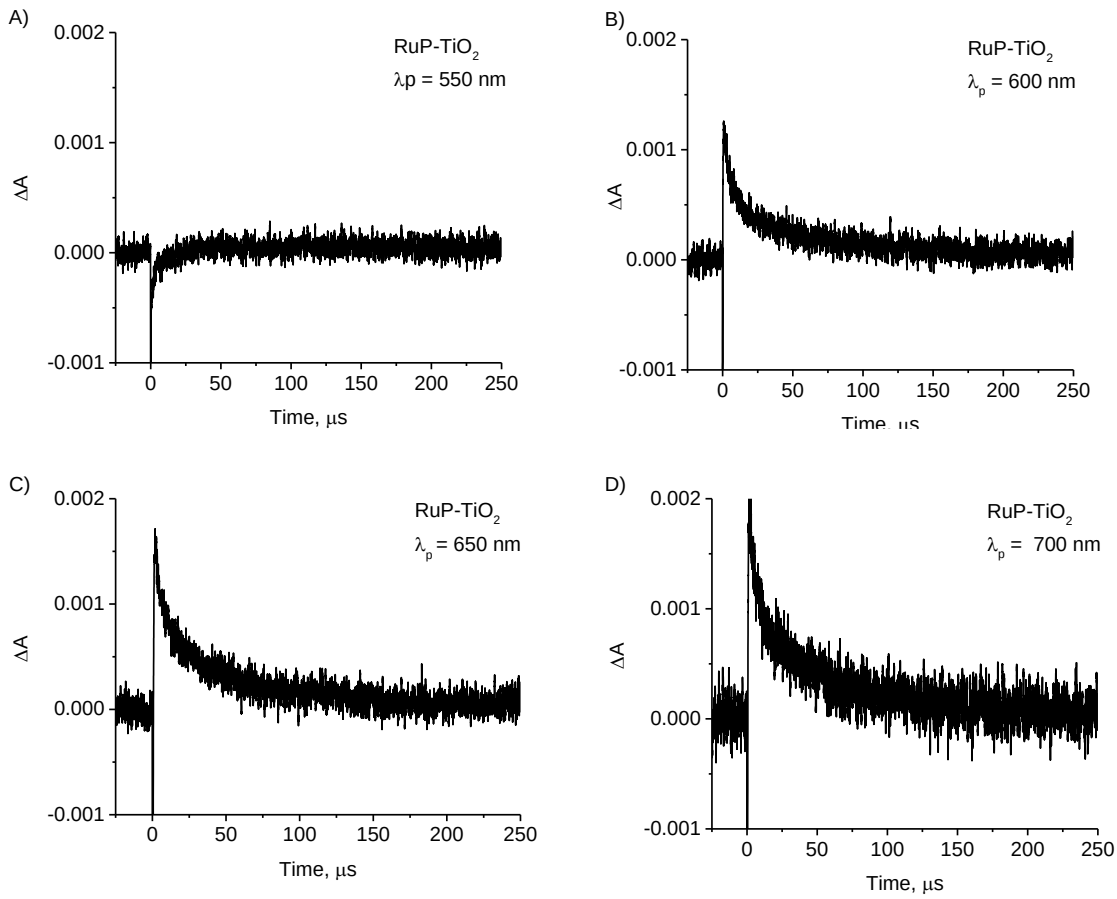

Figure S15. Kinetics at A) 550 nm, B) 600 nm, C) 650 nm and D) 700 nm obtained in flash photolysis for the RuP-TiO_2 samples in Na_2SO_4.

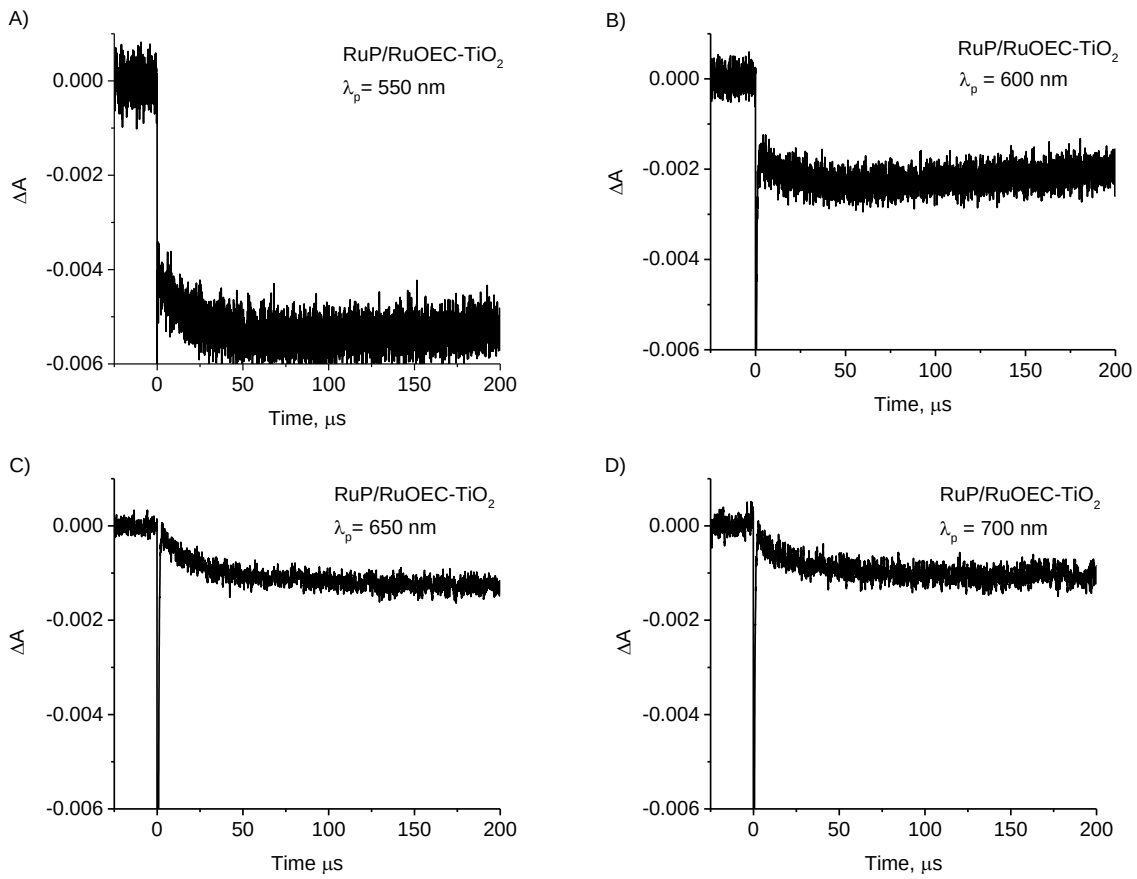

Figure S16. Kinetics at A) 550 nm, B) 600 nm, C) 650 nm and D) 700 nm obtained in flash photolysis for the RuP/RuOEC-TiO_2 samples in phosphate buffer.

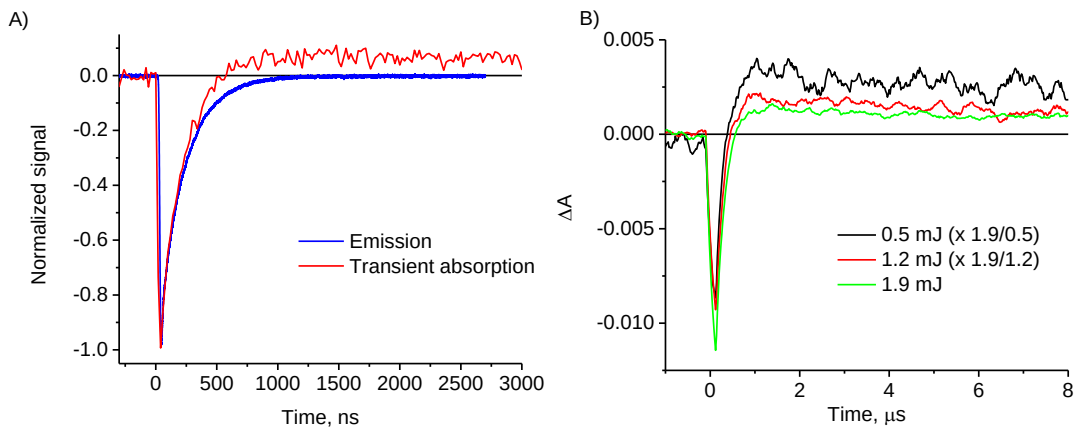

Figure S17. A) Comparison of pure emission (measured without probe) and transient absorption for RuP-TiO_2 in HCl electrolyte (pump energy 1.9 mJ). B) Kinetics at 700 nm for the RuP-TiO_2 in HCl recorded at different pump energy. The amplitudes of those at smaller pump energies (0.5 mJ and 1.2 mJ) were multiplied with the factors indicated in the legend.

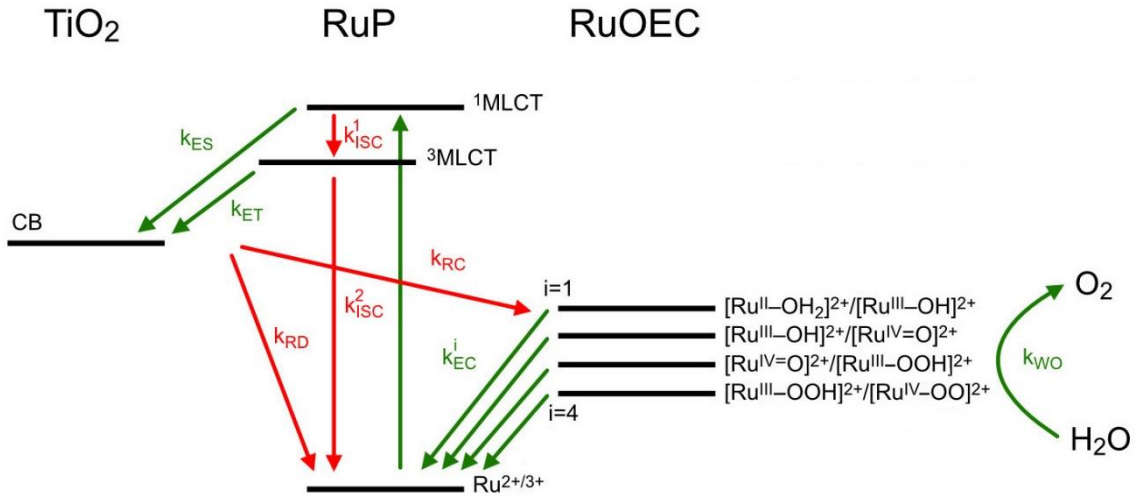

Scheme S1. Energetic scheme of the RuP/RuOEC-TiO_2 system with arrows showing desired (green) and competing undesired (red) electron transfer processes. The given rate constants correspond to the following processes: k_{ES} – electron injection from the singlet state of RuP, k_{ET} – electron injection from triplet state of RuP, k_{ISC}^1 – intersystem crossing from ^{1}MLCT to ^{3}MLCT, k_{ISC}^1 – intersystem crossing from ^{3}MLCT to the ground state, k_{EC}^i – electron transfer from different oxidized states of RuOEC to RuP, k_{WO} – water oxidation, k_{RD} – electron recombination between TiO_2 and the dye (RuP), k_{RC} – electron recombination between TiO_2 and the catalyst (RuOEC).

Comment to the scheme:

The total charge separation efficiency is a product of partial charge separations: electron injection (ϕ_{INJ}), RuP regeneration from different oxidation states of RuOEC (ϕ_{REG}^i), and water oxidation efficiency at the catalyst (ϕ_{WO}):

$$\phi = \phi_{INJ} \times \prod_{i=1}^{n} \phi_{REG}^{i} \times \phi_{WO} = \left(1 - \frac{k_{ISC}^1}{k_{ES} + k_{ISC}^1} \times \frac{k_{ISC}^2}{k_{ET} + k_{ISC}^2}\right) \times \prod_{i=1}^{n} \frac{k_{EC}^i}{k_{EC}^i + k_{RD}} \times \frac{k_{WO}}{k_{WO} + k_{RC}}$$

From our femtosecond transient absorption and flash photolysis experiments, the following rate constants can be deduced: $k_{ES} + k_{ISC}^1 \geq (0.3\ \text{ps})^{-1}$; k_{ET} = from $(300\ \text{ps})^{-1}$ to $(10\ \text{ps})^{-1}$; k_{RD} = from $(70\ \mu\text{s})^{-1}$ to $(45\ \mu\text{s})^{-1}$; $k_{EC}^1 = (70\ \text{ps})^{-1}$. Therefore, the efficiency of electron injection from RuP and the efficiency of dye regeneration from the lowest oxidation states of RuOEC (i=1) should be close to 100%. The relatively low photocurrents of the system are probably due to too slow regeneration rates from the high-valent metal-oxo species (especially i=3,4) with respect to k_{RD} and/or too slow water oxidation (k_{WO}) with respect to electron recombination to the catalyst (k_{RC}). The total water oxidation rate (k_{WO}) is equal to turnover frequency, which has been reported to be around 0.2 s^{-1} for similar catalyst.[1] However, the rate constants of other slow processes could not be determined in our experiments.

(1) Tong, L.; Thummel, R. P. Mononuclear Ruthenium Polypyridine Complexes That Catalyze Water Oxidation. *Chem. Sci.* **2016**, *7* (11), 6591–6603.